Am J Transl Res 2020;12(1):54-69
www.ajtr.org /ISSN:1943-8141/AJTR0103642

Original Article

Neuropathic pain releasing calcitonin gene related peptide protects against stroke in rats

Yida Wang[1], Zhenxiu Liu[2], Xinyu Ge[3], Xinyu Hu[4], Xiangyuan Cao[1], Lei Li[1], Jianhua Xia[5], Fulong Li[4], Liang Gao[1]

[1]Department of Neurosurgery, Shanghai Tenth People's Hospital, Tongji University School of Medicine, Shanghai 200072, China; [2]Department of Anesthesiology, The First Affiliated Hospital of Suzhou University, Suzhou 215006, Jiangsu, China; [3]Department of Cardiovascular Surgery, Shanghai East Hospital, Tongji University School of Medicine, Shanghai 200120, China; [4]Department of Anesthesiology, The First Affiliated Hospital of Hebei North University, Hebei North University, Zhangjiakou 075000, Hebei, China; [5]Department of Anesthesiology, Shanghai Pudong New District People's Hospital, Shanghai 201299, China

Received October 17, 2019; Accepted December 17, 2019; Epub January 15, 2020; Published January 30, 2020

Abstract: Neuropathic pain (NPP) is deemed as a potential risk of stroke; however, recent pieces of evidence showed that calcitonin gene-related peptide is involving in pain progression as well as organ protection. The mechanisms underlying the neuroprotection of calcitonin gene-related peptide are yet poorly described with respect to stroke. The present study showed that the elevated level of calcitonin gene-related peptide-induced by NPP exerts a protective effect against stroke in rats, which was further confirmed in vivo and vitro via mitigation of inflammatory response, inhibition of neuronal cell apoptosis, and increase in regional cerebral blood flow. Repetitive transcranial magnetic stimulation at trigeminal ganglion was performed to simulate to facilitate the release of calcitonin gene-related peptide for a similar neuroprotective effect. Together, these findings posit that the release of calcitonin gene-related peptide-induced by NPP or repetitive transcranial magnetic stimulation protects against stroke in rats. Thus, repetitive transcranial magnetic stimulation could have high application prospects for the prevention and treatment of stroke.

Keywords: Neuropathic pain, calcitonin gene related peptide, stroke, repetitive transcranial magnetic stimulation

Introduction

Stroke is also known as ischemic stroke and hemorrhagic stroke and the second leading cause that compromises the human species [1]. The ischemic stroke produces immediate neurological deficits and massive cerebral infarction, which leads to neuronal cell death, exacerbating blood-brain barrier damage, microvascular failure, and brain edema, eventually causing death and disability [2]. Numerous modifiable risk factors, such as hypertension, diabetes mellitus, dyslipidemia, and inflammation, are responsible for stroke [3]. Hypertension has been associated with hemorrhagic stroke and also contributes to atherosclerotic disease, which can also initiate ischemic stroke [4]. Chronic pain is widely recognized to impact blood pressure and is associated with an increased risk of hypertension [5]. However, the correlation between pain and stroke is not yet clarified.

Neuropathic pain (NPP) is a lesion affecting the somatosensory system that leads to a long-term debilitating condition, thereby declining the quality of life. A series of pathophysiological changes of NPP cause patients to suffer anxiety, depression, and elevated blood pressure [6]. Nevertheless, recent evidence demonstrated that various NPP-related molecules, including calcitonin gene-related peptide (CGRP) and adenosine (ADO) are involved in pain progression as well as organ protection [7, 8]. Therefore, studies evaluating the correlation between NPP and stroke occurrence and severity were warranted. Previous studies also indicated that inflammatory responses after a stroke have a pivotal role in secondary brain injury and other pathophysiological consequences [9]. Additionally, the transformation of focal inflammation to global inflammation might continuously shape the evolving pathological process and directly affect the clinical outcome of patients [3]. Although the study of the pathological pro-

cess is well documented, the neuroprotection in stroke remains a conundrum that has not been elucidated unequivocally.

Herein, we examined the effect of long-term NPP established through nerve chronic constriction injury (CCI) on ischemic stroke rats and stroke-prone spontaneously hypertensive (SHRSP) rats. Surprisingly, the neuroprotective effects of NPP on stroke rats further demonstrated that the protective effect was predominantly attributed to the release of CGRP, which was accompanied by changes in pro-inflammatory cytokines, neuronal apoptosis, and regional cerebral blood flow (rCBF). Finally, the repetitive transcranial magnetic stimulation (rTMS) was manipulated at the trigeminal ganglion with similar neuroprotection, which provided the potential value of the clinical practice.

Materials and methods

Study design

The present study was designed to characterize the effects of NPP on stroke in vitro and in vivo and further investigate the potential mechanism. The initial research focused on the phenotype of rats subjected to chronic constriction injury to the left infraorbital nerve (CCI-ION), then compared the infarction volume after middle cerebral artery occlusion (MCAO) injury. SHRSP rats were further used to confirm the neuroprotective effects, including the observation of demyelinating neuropathy and survival rate. Then, as potential effectors, ADO and CGRP were selected and detected for further study. The expression of inflammatory cytokines, apoptosis of neuronal cells and regional blood flow were measured to characterize the potential mechanism. Finally, stimulation of trigeminal ganglion with rTMS was also administrated to confirm whether the protective effect consistently exists.

Animals

All the animal experiments were approved by the Institutional Animal Care and Use Committee of The Second Military Medical University. Healthy male Sprague-Dawley (SD) rats (6-8 weeks) and SHRSP (8-12 weeks) rats were supplied by the Experimental Animal Center of The Second Military Medical University. All the rats were housed in a temperature-controlled facility (25 ± 1°C) on a 12 h light-dark cycle. Food and water were provided ad libitum. After 2 weeks acclimatizing to the vivrium, the experiments were conducted in accordance with institutional guidelines of Second Military Medical University for health and care of experimental animals. SHRSP rats were administrated with 8% high salt diet 20 d after CCI-ION. All rats were randomized to groups, the whole process was blinded to operators who perform the MCAO.

NPP model of CCI-ION

Rats were anesthetized by intraperitoneal injection of pentobarbital sodium (10 mg/kg). A 0.5 cm incision was made at approximately 0.5 cm along the facio-nasal furrow of the rats on the left side of the face, below the zygomatic bone in the rats' cheeks. The subcutaneous tissues, muscle, and surrounding fascia were blunt separated to expose the infraorbital foramen. The infraorbital nerve traveled from the infraorbital foramen was observed in a fan-shape distribution. A glass dissecting needle was used to free the infraorbital nerve from the proximal end for approximately 4 mm. The infraorbital nerve was ligated using two pieces of absorbable thread (5-0 chromic catgut suture) under a microscope (about 2 mm spacing) around the nerve with proper strength to mainly form a constriction ring. The incision was sutured using 4-0 chromic catgut suture. In the sham operated rats, infraorbital nerve was exposed using the same method without any ligated. The entire operation was conducted under sterile condition. The operated rats were sent to cages after recovering from anesthesia on a warming pad.

Mechanic pain threshold and rCBF measurement

Behavioral reactions of the rats were tested one day before the CCI-ION surgery and every 10 d postoperatively using the Von-Frey flaments. The stimulation strengths were administrated from low to high (0.07, 0.16, 0.4, 0.6, 1.0, 1.4, 2.0, 4.0, 6.0, 8.0, 10.0 and 15.0 g, respectively). Each stimulation was tested five times on the bilateral whisker pads of the rats. The positive symptoms are as follows: (1) Dodge behaviors including backward movement, turning around or shaking the head to avoid the stimuli, the rats would curl their body, move

closer to the cage walls or hide their face and head under their body. (2) Scratching the stimulated region of the face more than three times. (3) Aggressive behaviors of grasping and biting the stimulating device. The mechanical pain threshold value was recorded if one or more symptoms were presented by the rats. rCBF in the middle cerebral artery (MCA) dominated area measured by Laser Doppler Flowmetry after MCAO has been completed.

Middle cerebral artery occlusion (MCAO) model establishment

40 d after NPP model establishment of SD rats, transient focal cerebral ischemia was induced by the intraluminal occlusion model as previously described [10]. SD rats were anesthetized with intraperitoneal injection of pentobarbital sodium (10 mg/kg). The left common carotid artery (CCA) and the external carotid artery (ECA) were exposed via a midline neck incision. A poly-L-lysine coated monofilament suture (Shadong Biotechnology Co. Ltd., Shanghai, China) was chosen according to the body weight of the rats. After inserted from the ECA into the internal carotid artery (ICA), the monofilament suture was gently advanced into the proximal anterior cerebral artery (18-20 mm from CCA bifurcation) to occlude the MCA. The incision was sutured using 4-0 chromic catgut suture with part of the monofilament suture exposed. Two hours later, the monofilament suture was pulled out to allow reperfusion for 22 h. Evaluation of neurological behavior was administrated 24 hours after MCAO, the brain and serum samples were collected for further analysis. Body core temperature was measured rectally and maintained at 37 ± 2°C with a heating pad and a heating lamp throughout the procedure.

Evaluation of neurological behavior

Zea Longa test was performed by a blinded observer to evaluate the neurological function after 24 h following MCAO. Neurological deficit was evaluated on a four-point scale (0-4) as previously described [11]. (0 = no deficit, 1 = failure to fully extend right forepaw, 2 = circling to the right side, 3 = falling to the right side, 4 = no spontaneous walking with a depressed level of consciousness).

Evaluation of infarction volume

Rats were sacrificed 24 h after MCAO, and the brain was removed immediately. Serial 2 mm thick coronal sections were prepared with a brain-cutting matrix (ASI Instruments, Warren, MI, USA), and immersed in 2% 2,3,5-triphenyltetrazolium chloride (TTC) solution (Sinopharm Chemical Reagent Co. Ltd., Shanghai, China) at 37°C for 30 min and then fixed with 4% phosphate-buffered formalin solution. Infarct size was calculated using ImageJ software (NIH, MD, USA) and corrected the possible interference of brain edema by subtracting the volume of the non-ischemic hemisphere from that of the ischemic hemisphere. These values were then multiplied by the thickness of the respective slices and summed to yield the total infarct volume. Infarct volume (%) = total infarct volume/total section volume × 100.

Microinjection of the drugs

Rats were fixed in a stereotaxic apparatus (Shanghai Alcott Biotech Co. Ltd., Shanghai, China) after anesthetized. Sterile vehicle (normal saline, NS), CGRP (4 ug/kg, Abcam, UK) or CGRP antagonist (CGRP8-37, 2 ug/kg; Sigma Aldrich, USA) were injected into the left cerebral cortex (1 mm anterior to the bregma and 2 mm left of the midline) in 30 min followed by MCAO operation. The injection velocity was 0.1 ul/min and the total volume was 1 ul. At the end of the injection, the micro injector was kept immobile for 10 min before withdrawal.

Repetitive transcranial magnetic stimulation (rTMS)

The center of the coil was in contact with the petrous portion of left temporal bone. During the stimulation, rats were tested while keep them restrained, awake and calm for real and sham stimulation. Repeated rTMS or sham stimulation was administrated for 7 d (twice/day) before MCAO and followed by 2 times stimulation during reperfusion. The rTMS treatment protocol for one time comprised ten 5 s strains at a rate of 20 Hz with a 55 s intertrain interval. The resting motor threshold (RMT) was defined as the lowest stimulator output when the peak-to-peak amplitude of motor evoked potentials was greater than 5% of its maximal amplitude in at least half of the 10 trials. The stimulation intensity was set at 100% of the average RMT [12, 13]. The sham treatment consisted of positioning the coil perpendicular to the scalp of the same area and using the same frequency and intensity sham stimulation.

Enzyme-linked immunosorbent assay (ELISA)

The TNF-α, IL-1β and CGRP concentration levels in serum and cerebral cortex were determined using ELISA kits (Westang Biotechnology Co. Ltd., Shanghai, China) according to the manufacturer's instructions, respectively.

Quantitative real time-PCR (RT-qPCR)

Total RNA of brain tissue and cells was prepared with the NucleoSpin RNA II kit (MACHEREY-NAGEL) according to the manufacturer's protocol. The expression levels of IL-1β, TNF-α, Bcl-2 and Bax were detected by RT-qPCR using a 7500 Real-Time PCR System (Applied Biosystems). The primer sequences were designed as follows: forward, 5'-TGAGAGGGAAATCGTGCGTGAC-3'; reverse, 5'-GCTCGTTGCCAATAGTGATGACC-3' (β-actin of rat); forward, 5'-ATCCCAAACAATACCCA-3'; reverse, 5'-CAACTATGTCCCGACCA-3' (IL-1β of rat); forward, 5'-CCCCAATCTGTGTCCTTCTAA-3'; reverse, 5'-TTCAGCGTCTCGTGTGTTTC-3' (TNF-α of rat); forward, 5'-ATGTGTGTGGGGAGCGTCAA-3'; reverse, 5'-CAGAGACAGCCAGGAGAAATCAAA-3' (Bcl-2 of rat); forward, 5'-CATGAAGACAGGGGCCTTTTTG-3'; reverse, 5'-TCAGCTTCTTGGTGGATGCGTC-3' (Bax of rat). All expression levels were normalized to β-actin gene expression levels.

Kluver-Barrera staining

The demyelinating neuropathy of SHRSP rats was shown with Kluver-Barrera staining. The hippocampal CA1 region of brain tissues were obtained 40 d after CCI-ION or sham operation. After washed in phosphate buffer 4 times (30 min each time) and dried overnight, slides were incubated in ddH_2O for 5 min and then dehydrated in 50% ethanol (EtOH) and 70% EtOH for 5 min each. Slides were placed in 0.1% luxol fast blue MBS solution in a 65°C water bath for 24 h. The samples were rehydrated in 95% EtOH, 70% EtOH, 50% EtOH, and ddH_2O (5 min each), and then placed in 0.05% lithium carbonate solution, aqueous for 12 min with constant agitation, followed by 70% EtOH (2 min), 70% EtOH (1 min), and 50% EtOH (1 min). After counterstained in 0.1% cresyl violet acetate solution, aqueous for 10 min, the tissues were dehydrated in 50% EtOH (2 min), 70% EtOH (2 min), 95% EtOH (2 times, 2 min/time), 100% EtOH (2 times, 2 min/time). The slides were placed in xylene (2 times, 2 min/time) and then coverslipped with Eukitt.

Immunohistochemistry

The brain tissues of MCAO rats were obtained for the immunohistochemical staining 22 h after reperfusion. Briefly, rats were sacrificed and perfused with 4% paraformaldehyde. The brains were removed and kept in 4% paraformaldehyde for 6 h, then immersed in 30% sucrose at 4°C for 4 d. After embedding in a mixture of 25% sucrose and OCT compound (Sakura Finetek, Torrance, CA), 15 um sections were cut on a cryostat. The avidin-biotin complex technique was used in the staining and haematoxylin was used for counterstaining. The primary antibodies were rabbit anti-rat Iba-1 (1:2000, Cell Signaling). Normal goat serum and absence of primary antibody were used as negative control.

High performance liquid chromatography (HPLC) and analysis

Adenosine content in brain tissues was measured by HPLC 40 d after CCI-ION. Brain tissues were homogenized in 0.1 M perchloric acid with probe sonication (Vibra-Cell, Sonics & Materials, CT, USA) and centrifuged at 12,000 rpm for 5 min. After sieved using a 4 mm 0.22 uM nylon syringe filter (MicroSolv Technology Corporation, NJ, USA), the supernatant was eluted on a reverse-phase column (3 mm × 250 mm i.d., Lichrospher-100, Merck, Philadelphia, PA, USA) with a particle size of 5 mm, at a flow rate of 0.4 mL/min using a mobile phase (215 mM KH_2PO_4, 2.3 mM tetrabutylammonium hydrogen sulfate and 4% acetonitrile) adjusted to pH 6 with KOH. A UV detector (D-UV 6000; Alltech, Deerfield, IL, USA) was used to detect the signals at 260 nm. The treatment of standard solutions was the same as the samples. All peak areas were within the linear range of the standard curves. The adenosine values were calculated from the linear regression curve based on standard solutions.

Cell culture

The BV-2 and PC12 cell line was purchased from Shanghai Institutes for Biological Sciences, Chinese Academy of Sciences. BV-2 cells were cultured in DMEM medium and PC12 cells were cultured in RPMI 1640 medium,

which was supplemented with 10% FBS, 100 U/mL of penicillin and streptomycin in a saturated humidified incubator (37°C, 5% CO_2; Thermo Fisher Scientific, MA, USA). The cells were allowed to grow for 24 h in the culture medium prior to treatment in all experiments.

Oxygen-glucose deprivation and reoxygenation (OGD/R) model and cell treatments

The BV-2 and PC12 cells were pretreated primarily with PBS or CGRP for 30 min, the cells were then incubated in glucose-free Earle's balanced salt solution (BSS) in the Billups-Rothenberg anaerobic chamber containing 95% nitrogen and 5% CO_2. The chamber was sealed and incubated for 2 h at 37°C. Cells were removed from the chamber and replaced with normal medium, normoxia and 5% CO_2 conditions at 37°C for 3 h. Control cells were incubated in a common medium under normal conditions during the entire experiment. Cells were then collected for further detection.

Flow cytometry

The cell death was detected by Annexin V/7AAD staining analysis (Annexin V staining for early apoptotic cells, and 7AAD staining for late apoptotic or necrotic cells). Alexa Fluor 488 labeled-Annexin V and 7AAD (Invitrogen) were used according to the manufacturer's instruction. Flow cytometric analysis was performed with a BD FACScalibur flow cytometer (BD FACSCalibur TM Flow Cytometer, USA) to count 5000 cells for each experiment.

Histopathological examination

After 22 h reperfusion, the MCAO rats were deeply anesthetized and perfused with 4°C phosphate-buffered saline (PBS), followed by 4% paraformaldehyde through the heart. Ischemic brain tissues in the hippocampal CA1 region of left hemisphere were obtained and fixed in 4% paraformaldehyde. After embedded in paraffin and cut for 5 um slice, hematoxylin-eosin (H&E) staining was performed according to the manufacturer's instructions.

Western blotting assay

The total protein from OGD/R cells was prepared with cold lysis buffer containing 1 mM phenylmethylsulfonyl fluoride according to the manufacturer's instructions. After boiled in 4× loading buffer, cell extract was subjected to SDS-PAGE and transferred onto the PVDF membranes (Millipore, USA). After blocking nonspecific binding sites for 1 h with 5% dried skim milk in TBS at 37°C, the membrane was incubated with primary antibodies against Bcl-2, Bax at 4°C overnight prior to incubation with IRDye800CW-conjugated secondary antibody (Rockland). The image was captured by the Odyssey infrared imaging system (Li-Cor Bioscience, Lincoln, NE, USA). The data were analyzed using ImageJ software (NIH). β-actin was used as loading control.

Statistical analysis

All the data were analyzed using statistical software SPSS 23.0 and expressed as means ± standard deviation. Differences among groups were determined using one-way ANOVA, followed by a post hoc LSD test. Comparisons between two groups were performed using a Student's t test. Survival rate was compared using Log-rank (Mantel-Cox) test. $P < 0.05$ were considered to be significant.

Results

Neuropathic pain protects against stroke in both ischemia-reperfusion and SHRSP rats

To investigate the influence of neuropathic pain on stroke model, CCI-ION was used in the present study (Figure S1). The neuropathic pain induced by CCI-ION lasted for about 80 d evaluated by pain threshold (Figure S2). After CCI-ION for 40 d, SD rats were subjected to MCAO for 2 h followed by 22 h reperfusion. Cerebral infarction and neurological deficit scores were evaluated by 2% TTC staining and Zea Longa score, respectively. In comparison with the sham-operated rats, CCI-ION rats have shown a smaller cerebral infarct volume (**Figure 1A** and **1B**) and the alleviated neurological deficit (**Figure 1C**). Such protective effect was consistent in rats subjected to chronic constriction injury to the sciatic nerve (CCI-SN) (Figure S3).

To further explore the role of neuropathic pain for stroke, CCI-ION was performed in SHRSP rats. The demyelinating neuropathy of SHRSP was shown with Kluver-Barrera staining 40 d after CCI-ION or sham operation. CCI-ION obviously mitigated the demyelinating neuropathy

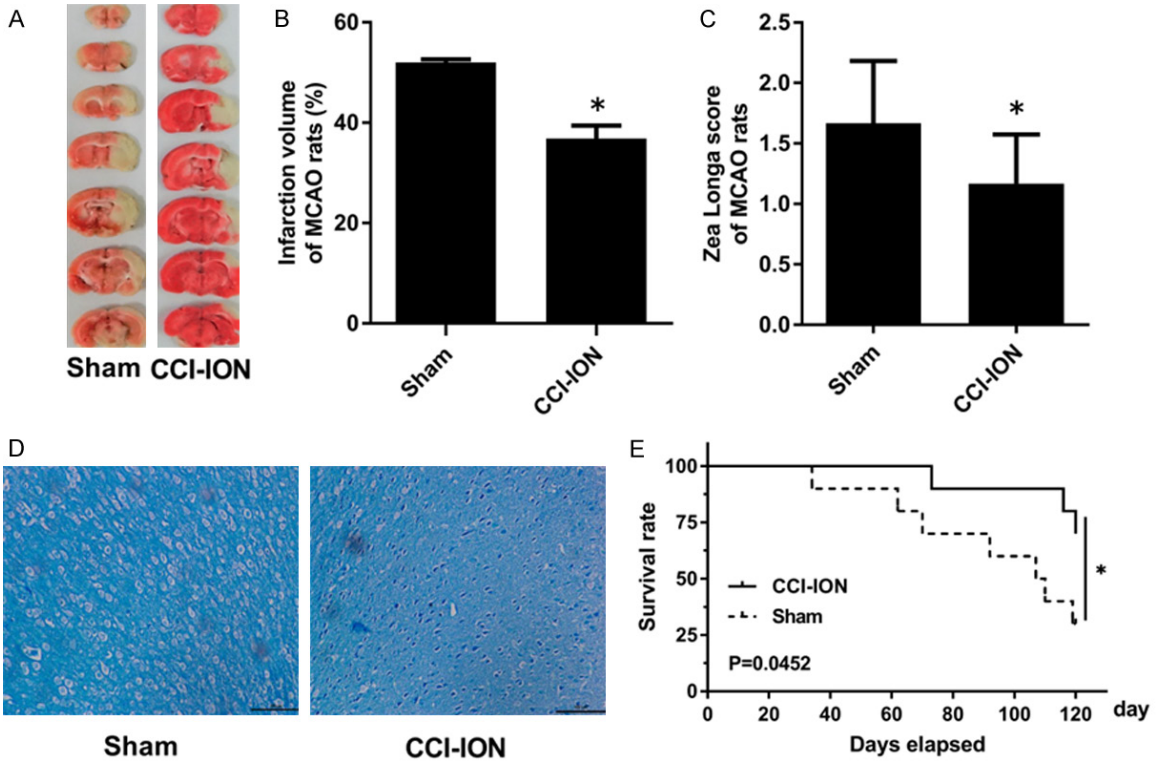

Figure 1. Neuropathic pain protects against stroke in both ischemia-reperfusion and SHRSP rats. (A, B) 2% TTC staining of coronal brain sections and quantitative analysis of the infarct volume were shown that CCI-ION significantly decreased the infarction volume than sham group. Areas of brain infarction appear white. n=5 rats. (C) Zea Longa score of the MCAO rats indicated rats in CCI-ION group had better neurological behavior than sham group, n=5 rats. (D) The demyelinating neuropathy was shown with Kluver-Barrera staining, rats in CCI-ION group suffer less demyelinating neuropathy than sham group, scale bar =100 um. (E) Longer survival rate of SHRSP rats had been found in CCI-ION group compared with sham group, n=10 rats. Data are shown as mean ± SD. Significance is determined by Student's t test (B, C) or Log-rank (Mantel-Cox) test (E). *P < 0.05 compared with sham group. TTC: 2,3,5-triphenyltetrazolium chloride; CCI-ION: chronic constriction injury to the left infraorbital nerve; MCAO: middle cerebral artery occlusion.

compared with sham group (**Figure 1D**). Moreover, 120 d survival rate of SHRSP model was significantly higher in CCI-ION group than sham group (**Figure 1E**).

CCI-ION induced neuroprotective effects were mediated by CGRP rather than ADO

The content of ADO in cortical tissues was measured by HPLC, but it was failed to show any significant difference between CCI-ION and sham group (Figure S5A and S5B). Pretreatment of 8-Cyclopentyl-1,3-dipropylxanthine (DPCPX), a selective high affinity antagonist ligand for A1 adenosine receptors dissolved in DMSO (5 mM), failed to abolish the effect of CCI-ION on cerebral injury induced by MCAO (Figure S5C-E). The results indicated that ADO may not participate in the protective effects of CCI-ION for stroke.

Another pain-related molecule, CGRP, was increased in cerebral cortex and serum of the rats subjected to CCI-ION for 40 d compared with sham group (**Figure 2A** and **2B**). CGRP was found difficult to pass through the vascular endothelium, to identify the effects of CGRP on ischemia-reperfusion injury, different doses of CGRP were microinjected into cerebral cortex 30 min before MCAO. Cortical microinjection of CGRP (4 ug/kg) 30 min before MCAO imitated the protective effects of CCI-ION and decreased the infarct volume. Preconditioning of CGRP8-37 30 min before MCAO largely attenuated the protective effects of CCI-ION in response to ischemic insults (**Figure 2C-E**). The protective effects were shown in a dose-dependent manner (Figures S6 and S7). To sum up, these results demonstrated CCI-ION induced neuroprotective effects were mediated by CGRP rather than ADO.

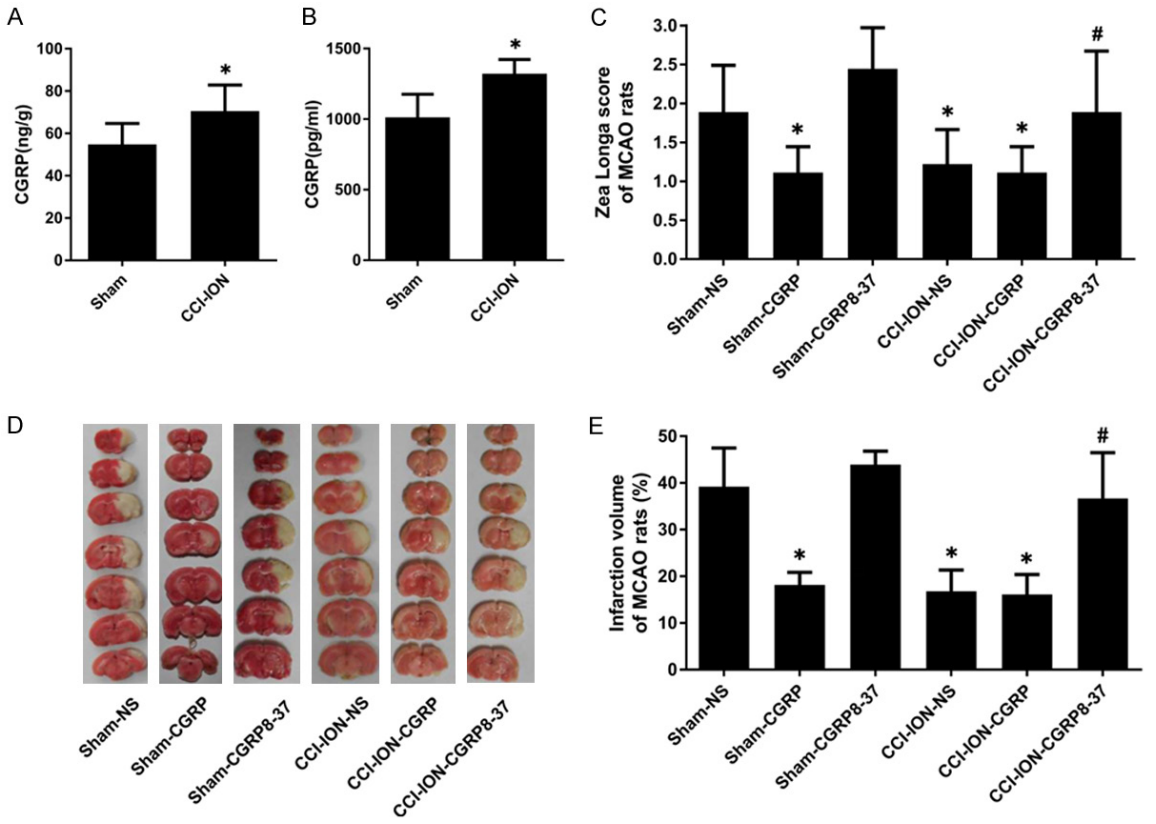

Figure 2. CCI-ION induced CGRP elevation protects against ischemic injuries. (A) The expression levels of CGRP in cortical tissues and (B) serum were elevated in rats subjected to CCI-ION for 40 days. n=5 rats. (C) 1 ul sterile NS, CGRP (800 ng/ul, 4 ug/kg) or CGRP8-37 (400 ng/ul, 2 ug/kg) were injected into cerebral cortex 30 min before MCAO in both CCI-ION and sham-operated rats. Zea Longa indicated CGRP treatment had similar protective effect with ICC-ION model, it alleviated neurological deficits when compared with sham group. n=5 rats. (D, E) 2% TTC staining of coronal brain sections and quantitative analysis of the infarct volume was shown that CGRP could substantially shrink the infarction volume compared with sham group, which was similar to CCI-ION model. n=5 rats. Data are shown as mean ± SD. Significance is determined by Student's t test (A, B) or ANOVA followed by LSD post-hoc testing (C, E). *$P < 0.05$ compared with sham or sham-NS group. #$P < 0.05$ compared with CCI-ION-NS group.

Neuroprotective mechanisms underlying the effects of CGRP mediate via mitigate inflammation and apoptosis

To investigate the potential neuroprotective mechanisms of CGRP, we detected the expression of inflammatory cytokines in cerebral cortex of MCAO rats 24 h after MCAO. Pretreatment of CGRP (4 ug/kg) decreased the expression of IL-1β and TNF-α in both mRNA and protein levels compared with NS group. In contrast, CGRP8-37 antagonized the effect and showed increased expression of IL-1β and TNF-α (**Figure 3A** and **3B**). Besides, immunohistochemical staining of Iba-1 indicated that CGRP pretreatment reduced the number of activated microglia compared with NS group (**Figure 3C**). The expressions of Bcl-2 and Bax were measured by RT-qPCR after MCAO followed by 22 h reperfusion to research the effect of CGRP on neuronal apoptosis. Increased Bcl-2 expression and decreased Bax expression in CGRP pretreatment compared with NS group and the reverse effect in CGRP8-37 group suggested that neuronal apoptosis could be attenuated via CGRP (**Figure 3D** and **3E**). Reduced blood supply in brain tissues is the major feature of stroke. We found CGRP pretreatment significantly augmented rCBF in the MCA dominated area, which measured by Laser Doppler Flowmetry after MCAO. CGRP8-37 pretreatment reduced the blood flow conversely (**Figure 3F**).

CGRP regulates inflammatory response of microglia and benefits neuron survival under oxygen-glucose deprivation and reoxygenation (OGD/R)

In cultured BV-2 cells, different doses of CGRP (0, 40, 80, 160 nM) were preconditioned 30

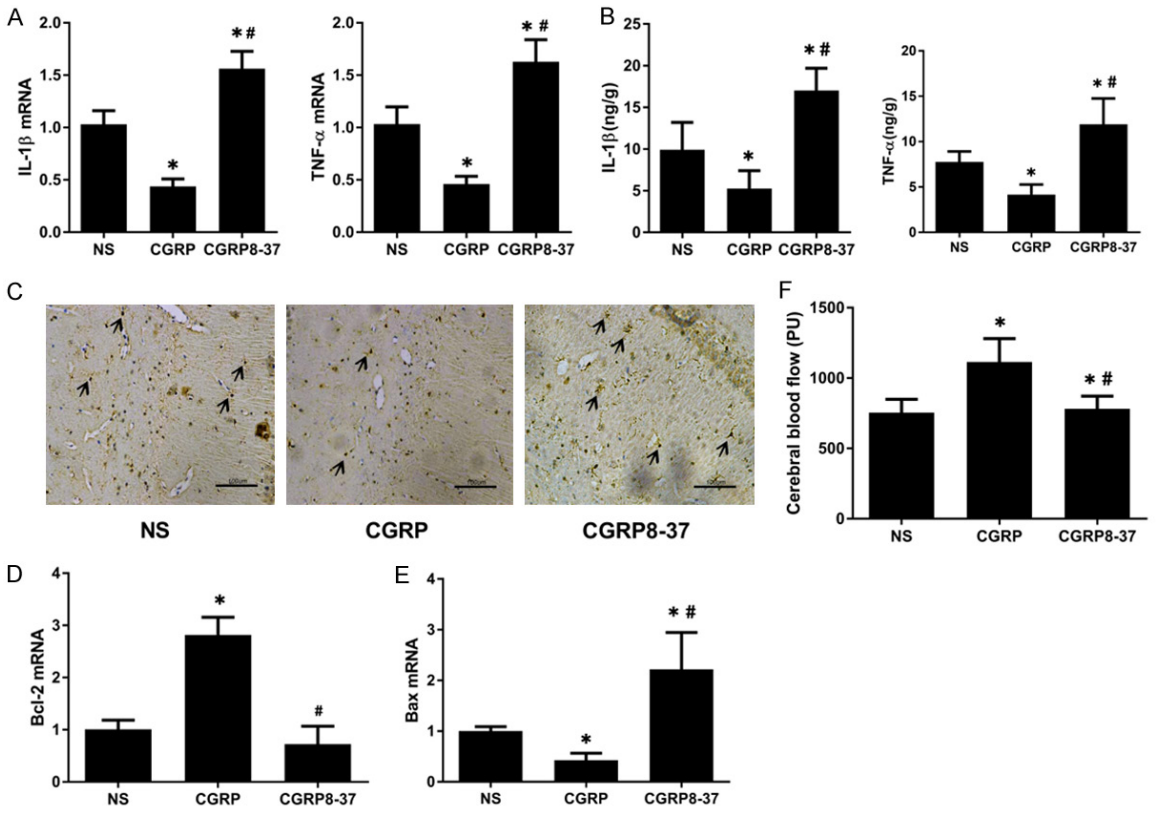

Figure 3. Protective effects of CGRP on cerebral injury induced by MCAO. A, B. The mRNA levels and protein level of IL-1β and TNF-α were expressed that CGRP pretreatment mitigated inflammatory response when compared with NS group, n=5 rats. C. Activated microglia (indicated by arrows) was shown by immunohistochemical staining of Iba-1, it was demonstrated that less microglia had been activated in CGRP group. Scale bar =100 um. D, E. Neuronal apoptosis was indicated by the mRNA levels of Bcl-2 and Bax. Increased Bcl-2 and decreased Bax suggested neuronal apoptosis was reduced after CGRP pretreatment, n=5 rats. F. CGRP pretreatment increased rCBF in the MCA dominated area, while CGRP8-37 could reverse the effect, n=5 rats. Data are shown as mean ± SD, and analyzed by ANOVA followed by LSD post-hoc testing. *P < 0.05 compared with NS group. #P < 0.05 compared with CGRP group. MCA: middle cerebral artery; rCBF: regional cerebral blood flow.

min before 2 hour's OGD and 3 hour's reoxygenation. The mRNA and protein levels of IL-1β and TNF-α were measured in BV-2 cells and the medium supernatant by RT-qPCR and ELISA, respectively. Pretreatment of CGRP significantly diminished the expression of IL-1β and TNF-α in a dose-dependent manner (**Figure 4A-D**). The results indicated that CGRP alleviated the inflammatory response of microglia underwent OGD/R. In cultured PC-12 cells, CGRP (160 nM) reduced the cell death induced by OGD/R as assessed by flow cytometric analysis of annexin V staining (**Figure 4E** and **4F**). The expression of Bcl-2 and Bax in PC-12 cells under OGD/R were measured by Western blot. CGRP pretreatment (160 nM) elevated the expression of Bcl-2 and reduced the expression of Bax (**Figure 4G** and **4H**). The results above indicated that CGRP pretreatment inhibited neuronal apoptosis and benefited neuron survival.

Neuroprotective mechanism of repetitive transcranial magnetic stimulation (rTMS) against stroke

Nociceptive stimulus targeting trigeminal nerve showed protective effects on stroke, however, the neuropathic pain induced by CCI-ION leads to physical and mental suffering. In order to test whether magnetic stimulation of trigeminal nerve system could protect against stroke, we introduced rTMS at trigeminal ganglion for stroke model in rats. SD rats were subjected to rTMS or sham stimulation for 7 d (twice/day) before MCAO followed by 2 times stimulation during reperfusion. Rats subjected to CCI-ION for 40 d before MCAO were served as positive

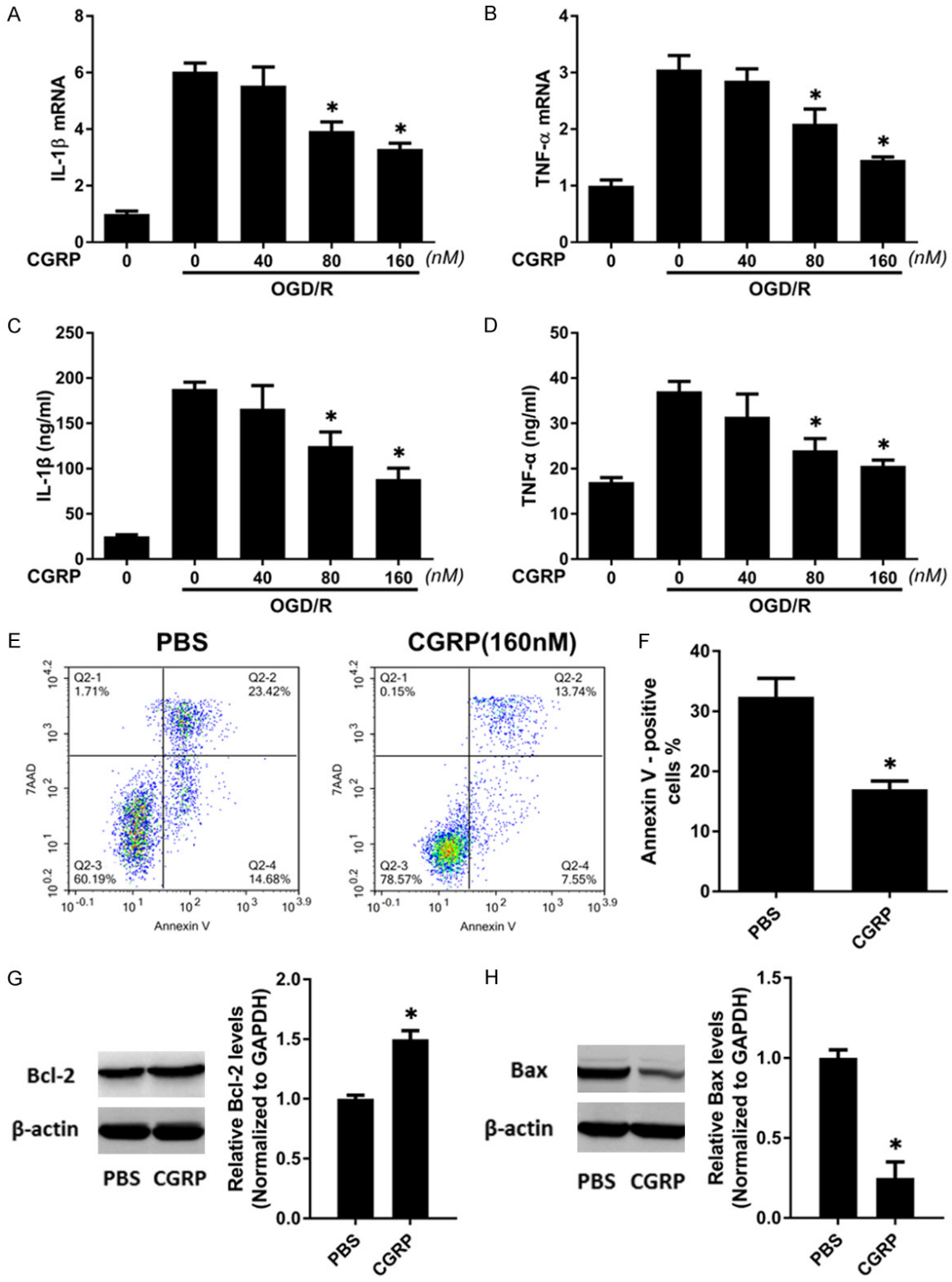

Figure 4. CGRP regulates inflammatory response of microglia and benefits neuron survival under OGD/R. (A-D) The mRNA levels and protein levels of IL-1β and TNF-α were measured after preconditioning with different doses of CGRP (0, 40, 80, 160 nM), it was indicated that CGRP mitigated inflammatory response of BV-2 in dose-dependent manner underwent OGD/R model, n=3. (E, F) The cell death of PC-12 cells was analyzed by flow cytometer (Annexin V and 7AAD staining), CGRP pretreatment (160 nM) reduced cell death compared with PBS group, n=3. (G, H) Immunoblotting and quantification analysis suggested neuronal apoptosis could be inhibited by CGRP pretreatment

(160 nM). Data are shown as mean ± SD. Significance is determined by ANOVA followed by LSD post-hoc testing (A-D) or Student's t test (F-H). *P < 0.05 compared with cells under OGD/R without CGRP preconditioning (A-D) or PBS group (F-H). OGD/R: Oxygen-glucose deprivation and reoxygenation.

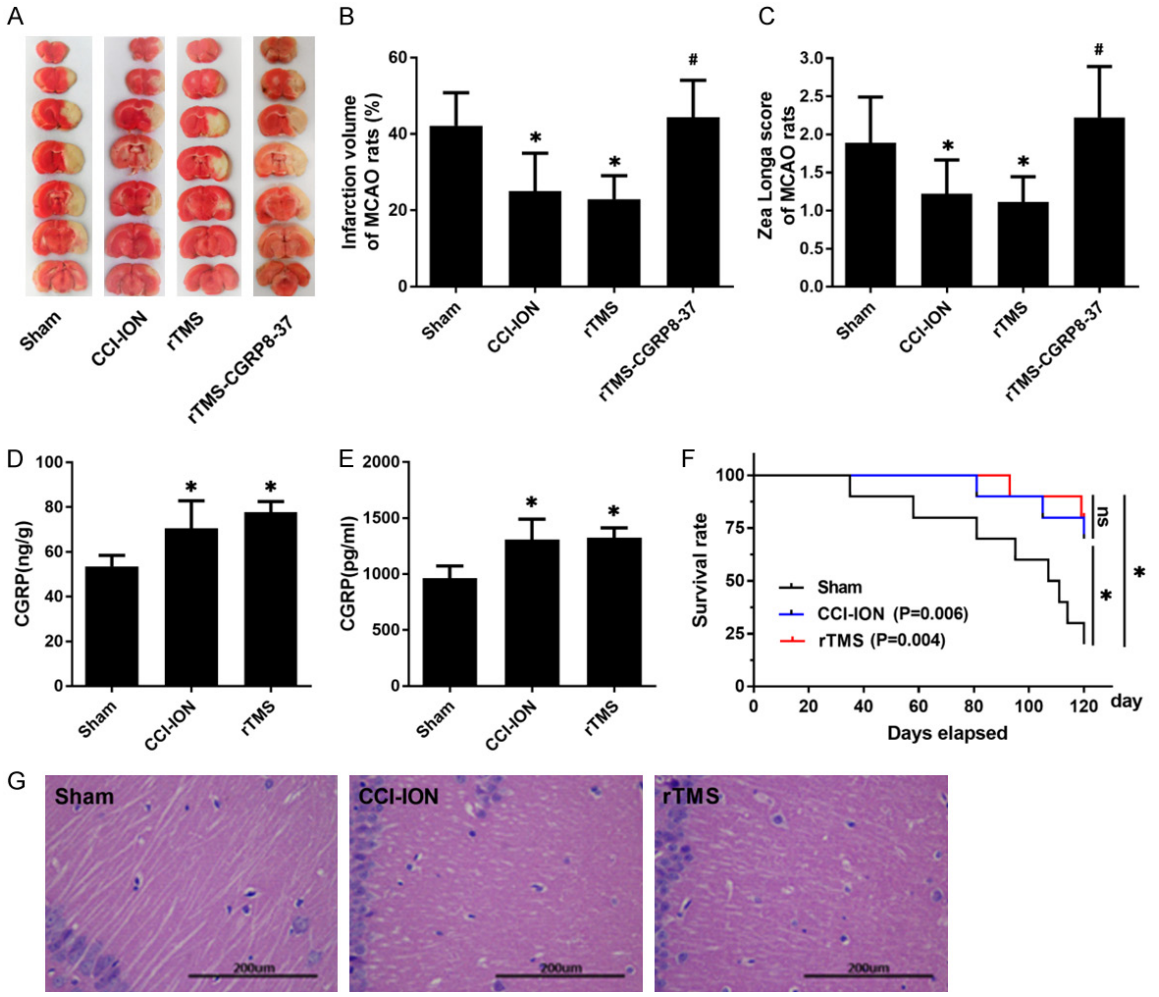

Figure 5. Repetitive transcranial magnetic stimulation (rTMS) protects against stroke in both ischemia-reperfusion and SHRSP rats. (A, B) 2% TTC staining of coronal brain sections and quantitative analysis of infarct volume and (C) Zea Longa score of the MCAO rats indicated rTMS had similar protective effect with CCI-ION model, CGRP8-37 could reverse the effect, n=5 rats. (D) The expression levels of CGRP in cortical tissues and (E) serum were elevated in rats subjected to CCI-ION and rTMS, n=5 rats. (F) Survival rate (120 days) of SHRSP rats shown that longer survival rate had been found in rTMS and CCI-ION group compared with sham group. n=10 rats. (G) The HE staining shown the pathological changes mitigated in CCI-ION and rTMS group when compared with sham group at day 40. Scale bar =200 um. Data are shown as mean ± SD. Significance is determined by ANOVA followed by LSD post-hoc testing (B-E) or Log-rank (Mantel-Cox) test (F). *P < 0.05 compared with sham group, #P < 0.05 compared with rTMS group.

control. Both infarct volume and neurological deficit were improved in rTMS treatment group (**Figure 5A-C**). Cortical microinjection of CGRP8-37 (400 ng/ul, 2 ug/kg) 30 min before MCAO significantly diminished the protective effects of rTMS (**Figure 5A-C**). Similar to CCI-ION, CGRP was also increased in cerebral cortex and serum of the rats subjected to rTMS for 7 days (**Figure 5D** and **5E**). To further identify the neuroprotective effects of rTMS, SHRSP rats were treated with rTMS at trigeminal ganglion twice/day for 80 d, successive rTMS treatment significantly improved survival rate of SHRSP rats (**Figure 5F**). The cerebral neuropathy is shown with HE staining in SHRSP rats after CCI-ION, rTMS (twice/day) or sham stimulation (twice/day). Neurological tissue disorganized and widening intercellular space was presented with

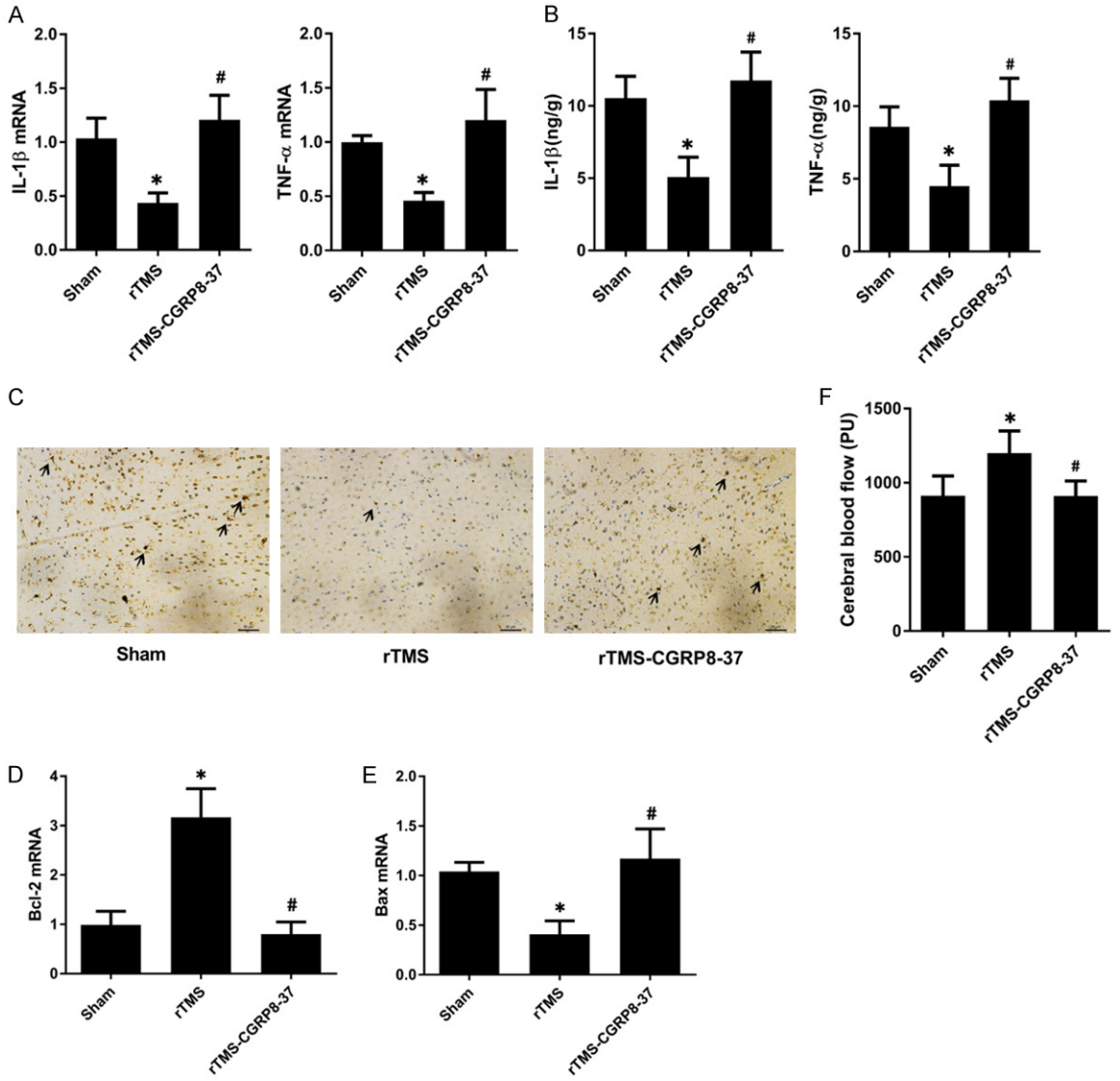

Figure 6. Neuroprotective mechanism of rTMS on cerebral ischemia-reperfusion injury. (A, B) The mRNA levels and protein levels of IL-1β and TNF-α were shown that rTMS alleviated the inflammatory response significantly compared with sham group, and CGRP8-37 could reverse the effect, n=5 rats. (C) Activated microglia (indicated by arrows) was shown by immunohistochemical staining of Iba-1, less microglia had been activated in rTMS group and CGRP8-37 could reverse the protective effect, scale bar =50 um. (D, E) Neuronal apoptosis was indicated by the mRNA levels of Bcl-2 and Bax. Increased Bcl-2 and decreased Bax suggested neuronal apoptosis was reduced after rTMS treatment compared with sham group, and CGRP8-37 could reverse the effect, n=5 rats. (F) Cerebral blood flow in MCA dominated area indicated that rTMS treatment increased rCBF, while CGRP8-37 could reverse the effect, n=5 rats. Data are shown as mean ± SD, and analyzed by ANOVA followed by LSD post-hoc testing. *P < 0.05 compared with Sham group. #P < 0.05 compared with rTMS group.

HE staining in sham group, while amelioration of these pathological changes were presented in CCI-ION and rTMS group (**Figure 5G**).

To further disclose the potential mechanism of rTMS on cerebral ischemia-reperfusion injury and identify whether CGRP is involved in the neuroprotective effects, SD rats were subjected to rTMS for 7 d (twice/day) before MCAO and 2 times rTMS during reperfusion. CGRP8-37 was injected 30 min before MCAO. The expression of inflammatory cytokines including IL-1β and TNF-α in cerebral cortex was significantly decreased in the rats received rTMS treatment compared with sham group. CGRP8-37 administration abolished the anti-inflammatory effects (**Figure 6A** and **6B**). Immunohistochemical staining of Iba-1 indicated that rTMS treatment

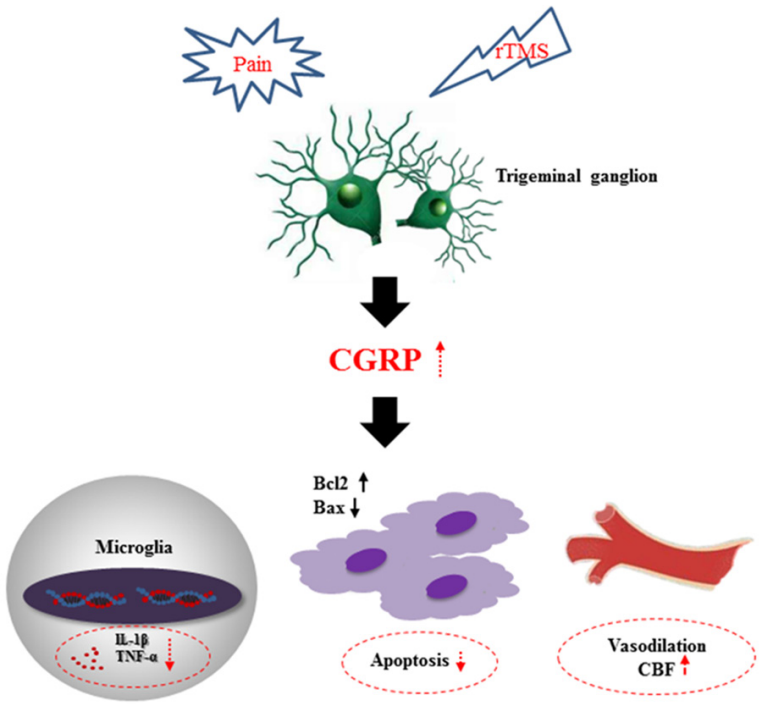

Figure 7. Schematic diagram of pain/rTMS induced neuroprotection against stroke.

reduced the number of activated microglia, the effect was also diminished by CGRP8-37 (**Figure 6C**). The influence of rTMS on neuronal apoptosis was detected by the expressions of Bcl-2 and Bax. Bcl-2 was highly expressed in rats treated with rTMS, and the expression of Bax was decreased. Inhibition of apoptosis was almost abolished when CGRP8-37 was administrated (**Figure 6D** and **6E**). Similarly, the augmentation of rCBF in the MCA dominated area was significantly increased by rTMS and reversed by CGRP8-37 (**Figure 6F**). The results together indicated that rTMS induced anti-inflammatory, anti-apoptosis and rCBF augmentation to protect against stroke, and CGRP played a key role in the neuroprotective effects of rTMS.

Discussion

Stroke is a major issue, and although the correlation between stroke and pain has been discussed, it is poorly described. The studies on NPP mainly concentrate on the formation of the nociceptive transduction pathway and damage-related impact. Accumulating evidence suggested that molecules involved in pain progress show in vivo and in vitro neuroprotective effects [14-17]. A double-edged effect makes it difficult to assert the influence of NPP on stroke. The present study was conducted to disclose the protective effects of NPP on the occurrence and severity of stroke. Herein, we showed that NPP reduced the infarct volume and improved the neurological behavior in rats suffering from MCAO. Unexpectedly, neuroprotective effects were still recognized in SHRSP rats, including demyelinating neuropathy alleviation and prolonged survival rate.

As pain-related molecules, ADO was reported to be involved in cerebral hypoxia tolerance [18], while CGRP was mainly stored at the end of the sympathetic nerve fiber and around the cerebral artery as a potential microvascular neuropeptide vasodilator [19]. The changes in CGRP and ADO demonstrated that the protective effects were mainly related to increased CGRP rather than ADO. CGRP mitigated the inflammatory response of activated microglia and benefited the survival of neurons in vivo and in vitro. Moreover, cerebral blood flow was also verified to be increased in MCAO rats with the application of CGRP. Continuous rTMS at trigeminal ganglion was successfully implemented to stimulate the trigeminal nerve system in order to trigger the effects of the NPP model; protective effects were observed in both ischemic stroke rats and SHRSP rats. Notably, CGRP plays a crucial role in the cerebral protection of stroke.

Typically, the pain has been linked to detrimental effects. A previous population-based follow-up study showed that the possibility of stroke significantly increases in patients with trigeminal neuralgia [20]. Nevertheless, the majority of patients with trigeminal neuralgia exhibit various comorbidities, such as hypertension, hyperlipidemia, and coronary heart disease. Additionally, the information about the medical history of smoking, alcohol intake, drug abuse, body mass index, and physical activity was not

provided, which might obscure the assessment of the risk of stroke. As a single factor, the significant role of NPP has been found to modulate the inflammatory response [21-23]. Moreover, neuroglobin carries oxygen and protects the brain from experimental stroke; this capacity was increased in cerebrospinal fluid of females suffering from chronic pain [24, 25]. Although the mechanisms underlying these findings have not been elucidated, the potential protective role of pain needs to be investigated further. Interestingly, animal studies revealed that squid suffering long-term hyperalgesia after a bodily injury has enhanced the physical ability to escape from predation [26]. Accumulating evidence indicated that pain is a warning signal that might boost the activation of the defense system of the body and produce preprotective effects.

In the current study, CCI-ION and CCI-SN are typically used as NPP models. Although the model does not represent assorted types of pain, it was still desirable due to the simulation of the most common vascular compressive neuralgia in humans. NPP was characterized by concomitant hyperalgesia, allodynia, and long-term pain, which had been successfully observed in the CCI model. The pain threshold in a model reaches the lowest level in a couple of days after the operation, is maintained for several weeks, followed by gradual recovery. All the tests were conducted during this period. It was observed that the CCI-ION group of SHRSP rats had higher survival rate within 120 d as compared to the sham group; however, the difference did not reach statistical significance in 145-d survival rate (Figure S4). This phenomenon could be attributed to the decreased CGRP level during gradual recovery, which was after 80 d post-CCI-ION operation (Figure S2). The high-salt diet was widely administered in various experiments; it promotes earlier stroke attack in rats [27, 28]. In the present study, 8% was chosen for the high-salt diet as it is suitable for long-term observation of the effects of NPP. This pilot study showed that CCI-ION-induced mean arterial pressure substantially increased in the first 10 days and gradually normalized around on day 20. In order to avert the peak blood pressure induced by CCI-ION, the high-salt diet was postponed for a couple of days after CCI-ION or rTMS in the present study.

CGRP is an important neurotransmitter and primarily localized to C and Aδ sensory fibers [19], and plays a major role in pain-induced neuroprotection in this study. CGRP synthesis is known to be upregulated in models of nerve damage. The molecule can be released together with the P substance to the peripheral tissues induced by chronic pain [29]. This accords with our observation that CGRP is increased in the cerebral cortex and the serum of the rats subjected to CCI-ION. For the potential positive effects, CGRP might benefit the physiological response to ischemia in several organs, including the heart, intestine, and kidney [30-32]. The mechanisms that trigger ischemia-reperfusion damages and secondary injuries are complicated, including global inflammation, mitochondrial dysfunction, overproduction of free radicals, neural necrosis, and apoptosis [3, 33, 34]. The upregulation of endogenous neuroinflammation and the transformation of focal inflammation to global inflammation facilitates neurological damage following the initial episode of ischemic stroke. Similarly, the current findings indicated that CCI-ION promotes CGRP release, thereby suppressing the activation of microglia and mitigating the post-stroke inflammatory response. Then, apoptosis within the ischemic penumbra, which occurs after several hours of the stroke, may contribute to a significant proportion of neuronal death [35]. In this study, CGRP significantly inhibited apoptosis via enhancing the expression of Bcl-2 and decreasing that of Bax. Also, flow cytometric analysis using annexin V staining demonstrated that CGRP reduces the cell death induced by OGD/R in vitro. Moreover, the major cardiovascular activity of CGRP is a potent vasodilator in physiological conditions [36]. Herein, CGRP pretreatment significantly augmented rCBF in the MCA-dominated area, which protects against ischemic injury in the early stage.

In order to simulate the protective effect of NPP on stroke and develop a potential strategy in clinical practice, rTMS, a new frontier in the treatment of neuropsychiatric maladies, was introduced in the present study. Recent reports show that high-frequency rTMS (20 Hz) triggers the expression of brain-derived neurotrophic factor (BDNF) in several brain areas in rats to improve the post-stroke depression outcome in patients [37]. Moreover, preconditioning with rTMS was demonstrated to produce an anti-apoptotic effect in the rat model of transient cerebral ischemia [38]. Intriguingly, the center of the coil was in contact with the cerebral cor-

tex of the rats. In this study, continuous rTMS at trigeminal ganglion led to increased CGRP in the cerebral cortex and serum, reduced the infarct volume and neuronal apoptosis (**Figure 7**), improved the neurological outcome of ischemic rats, and prolonged the survival rate of SHRSP rats. The safety and therapeutic effects of rTMS have been verified in the sundry diseases [37-39]. The neuroprotection in the present study predicts that continuous rTMS could be a promising therapy for stroke patients or patients with a high risk of stroke.

One fly-in-the-ointment in the study, the protective mechanism of CGRP on hemorrhagic stroke, also known as the SHRSP rat model, is not as well-established as the ischemic model. Also, the prolonged survival rate and improved demyelinating neuropathy staining need to be supplemented with a molecular basis to support this phenotype in order to confirm the function of CGRP on hemorrhagic stroke.

Conclusions

The current study delineated that the CGRP release induced by NPP protects against stroke in vivo and in vitro. The application of rTMS at trigeminal ganglion produces similar neuroprotective effects via the mitigation of inflammatory responses, inhibition of apoptosis, and improvement of rCBF. An understanding of the pain-related protective mechanism is crucial for developing novel approaches for stroke therapy.

Acknowledgements

We would like to thank Prof. Weizhong Wang for study design suggestion and technical assistance, to thank Dr. Yu Song and Dr. Songyu Chen for surgical assistance with stroke model. This work was supported by Scientific Research Program of Shanghai Science and Technology Committee (18411951300) and its sub-project (18411951301), Clinical research and cultivation project of Shanghai Shenkang Hospital Development Center (SHDC12017X17).

Disclosure of conflict of interest

None.

Address correspondence to: Liang Gao, Department of Neurosurgery, Shanghai Tenth People's Hospital, Tongji University School of Medicine, 301 Yanchang Road, Jing'an District, Shanghai 200072, China. Tel: +86-13817934652; E-mail: lianggaoh@126.com; Fulong Li, Department of Anesthesiology, The First Affiliated Hospital of Hebei North University, Hebei North University, 12 Changqing Road, Zhangjiakou 075000, Hebei, China. Tel: +86-15530396568; E-mail: lifulong8915833@163.com

References

[1] Hankey GJ. Stroke. Lancet 2017; 389: 641-654.

[2] Urday S, Kimberly WT, Beslow LA, Vortmeyer AO, Selim MH, Rosand J, Simard JM and Sheth KN. Targeting secondary injury in intracerebral haemorrhage--perihaematomal oedema. Nat Rev Neurol 2015; 11: 111-122.

[3] Shi K, Tian DC, Li ZG, Ducruet AF, Lawton MT and Shi FD. Global brain inflammation in stroke. Lancet Neurol 2019; 18: 1058-1066.

[4] Boehme AK, Esenwa C and Elkind MS. Stroke risk factors, genetics, and prevention. Circ Res 2017; 120: 472-495.

[5] Bruehl S, Olsen RB, Tronstad C, Sevre K, Burns JW, Schirmer H, Nielsen CS, Stubhaug A and Rosseland LA. Chronic pain-related changes in cardiovascular regulation and impact on comorbid hypertension in a general population: the Tromso study. Pain 2018; 159: 119-127.

[6] Cragg JJ, Noonan VK, Noreau L, Borisoff JF and Kramer JK. Neuropathic pain, depression, and cardiovascular disease: a national multicenter study. Neuroepidemiology 2015; 44: 130-137.

[7] Lu CX, Qiu T, Liu ZF, Su L and Cheng B. Calcitonin gene-related peptide has protective effect on brain injury induced by heat stroke in rats. Exp Ther Med 2017; 14: 4935-4941.

[8] Kwilasz AJ, Green Fulgham SM, Ellis A, Patel HP, Duran-Malle JC, Favret J, Harvey LO Jr, Rieger J, Maier SF and Watkins LR. A single peri-sciatic nerve administration of the adenosine 2A receptor agonist ATL313 produces long-lasting anti-allodynia and anti-inflammatory effects in male rats. Brain Behav Immun 2019; 76: 116-125.

[9] Chamorro A, Dirnagl U, Urra X and Planas AM. Neuroprotection in acute stroke: targeting excitotoxicity, oxidative and nitrosative stress, and inflammation. Lancet Neurol 2016; 15: 869-881.

[10] Shi YW, Zhang XC, Chen C, Tang M, Wang ZW, Liang XM, Ding F and Wang CP. Schisantherin A attenuates ischemia/reperfusion-induced neuronal injury in rats via regulation of TLR4 and C5aR1 signaling pathways. Brain Behav Immun 2017; 66: 244-256.

[11] Bachour SP, Hevesi M, Bachour O, Sweis BM, Mahmoudi J, Brekke JA and Divani AA. Com-

parisons between Garcia, Modo, and Longa rodent stroke scales: optimizing resource allocation in rat models of focal middle cerebral artery occlusion. J Neurol Sci 2016; 364: 136-140.
[12] Gao F, Wang S, Guo Y, Wang J, Lou M, Wu J, Ding M, Tian M and Zhang H. Protective effects of repetitive transcranial magnetic stimulation in a rat model of transient cerebral ischaemia: a microPET study. Eur J Nucl Med Mol Imaging 2010; 37: 954-961.
[13] Yoon KJ, Lee YT and Han TR. Mechanism of functional recovery after repetitive transcranial magnetic stimulation (rTMS) in the subacute cerebral ischemic rat model: neural plasticity or anti-apoptosis? Exp Brain Res 2011; 214: 549-556.
[14] Liu Z, Liu Q, Cai H, Xu C, Liu G and Li Z. Calcitonin gene-related peptide prevents blood-brain barrier injury and brain edema induced by focal cerebral ischemia reperfusion. Regul Pept 2011; 171: 19-25.
[15] Morancho A, Ma F, Barcelo V, Giralt D, Montaner J and Rosell A. Impaired vascular remodeling after endothelial progenitor cell transplantation in MMP9-deficient mice suffering cortical cerebral ischemia. J Cereb Blood Flow Metab 2015; 35: 1547-1551.
[16] Adebiyi MG, Manalo J, Kellems RE and Xia Y. Differential role of adenosine signaling cascade in acute and chronic pain. Neurosci Lett 2019; 134483.
[17] Huie JR, Garraway SM, Baumbauer KM, Hoy KC Jr, Beas BS, Montgomery KS, Bizon JL and Grau JW. Brain-derived neurotrophic factor promotes adaptive plasticity within the spinal cord and mediates the beneficial effects of controllable stimulation. Neuroscience 2012; 200: 74-90.
[18] Cui M, Bai X, Li T, Chen F, Dong Q, Zhao Y and Liu X. Decreased extracellular adenosine levels lead to loss of hypoxia-induced neuroprotection after repeated episodes of exposure to hypoxia. PLoS One 2013; 8: e57065.
[19] Russell FA, King R, Smillie SJ, Kodji X and Brain SD. Calcitonin gene-related peptide: physiology and pathophysiology. Physiol Rev 2014; 94: 1099-1142.
[20] Pan SL, Chen LS, Yen MF, Chiu YH and Chen HH. Increased risk of stroke after trigeminal neuralgia--a population-based follow-up study. Cephalalgia 2011; 31: 937-942.
[21] Ellis A and Bennett DL. Neuroinflammation and the generation of neuropathic pain. Br J Anaesth 2013; 111: 26-37.
[22] Fan Y, Ding S, Sun Y, Zhao B, Pan Y and Wan J. MiR-377 regulates inflammation and angiogenesis in rats after cerebral ischemic injury. J Cell Biochem 2018; 119: 327-337.
[23] Trevisan G, Benemei S, Materazzi S, De Logu F, De Siena G, Fusi C, Fortes Rossato M, Coppi E, Marone IM, Ferreira J, Geppetti P and Nassini R. TRPA1 mediates trigeminal neuropathic pain in mice downstream of monocytes/macrophages and oxidative stress. Brain 2016; 139: 1361-1377.
[24] Simon R. Neuroglobin: neuroprotection and neurogenesis. Neurosci Lett 2013; 549: 1-2.
[25] Raida Z, Hundahl CA, Nyengaard JR and Hay-Schmidt A. Neuroglobin over expressing mice: expression pattern and effect on brain ischemic infarct size. PLoS One 2013; 8: e76565.
[26] Crook RJ, Hanlon RT and Walters ET. Squid have nociceptors that display widespread long-term sensitization and spontaneous activity after bodily injury. J Neurosci 2013; 33: 10021-10026.
[27] Herisson F, Zhou I, Mawet J, Du E, Barfejani AH, Qin T, Cipolla MJ, Sun PZ, Rost NS and Ayata C. Posterior reversible encephalopathy syndrome in stroke-prone spontaneously hypertensive rats on high-salt diet. J Cereb Blood Flow Metab 2019; 39: 1232-1246.
[28] Rubattu S, Stanzione R, Bianchi F, Cotugno M, Forte M, Della Ragione F, Fioriniello S, D'Esposito M, Marchitti S, Madonna M, Baima S, Morelli G, Sciarretta S, Sironi L, Gelosa P and Volpe M. Reduced brain UCP2 expression mediated by microRNA-503 contributes to increased stroke susceptibility in the high-salt fed stroke-prone spontaneously hypertensive rat. Cell Death Dis 2017; 8: e2891.
[29] Del Fiacco M, Quartu M, Boi M, Serra MP, Melis T, Boccaletti R, Shevel E and Cianchetti C. TRPV1, CGRP and SP in scalp arteries of patients suffering from chronic migraine. J Neurol Neurosurg Psychiatry 2015; 86: 393-397.
[30] Tullio F, Penna C, Cabiale K, Femmino S, Galloni M and Pagliaro P. Cardioprotective effects of calcitonin gene-related peptide in isolated rat heart and in H9c2 cells via redox signaling. Biomed Pharmacother 2017; 90: 194-202.
[31] Magierowski M, Jasnos K, Sliwowski Z, Surmiak M, Krzysiek-Maczka G, Ptak-Belowska A, Kwiecien S and Brzozowski T. Exogenous asymmetric dimethylarginine (ADMA) in pathogenesis of ischemia-reperfusion-induced gastric lesions: interaction with protective nitric oxide (NO) and calcitonin gene-related peptide (CGRP). Int J Mol Sci 2014; 15: 4946-4964.
[32] Mizutani A, Okajima K, Murakami K, Mizutani S, Kudo K, Uchino T, Kadoi Y and Noguchi T. Activation of sensory neurons reduces ischemia/reperfusion-induced acute renal injury in rats. Anesthesiology 2009; 110: 361-369.
[33] Heger M, Reiniers MJ and van Golen RF. Mitochondrial metabolomics unravel the primordial trigger of ischemia/reperfusion injury. Gastroenterology 2015; 148: 1071-1073.

[34] Menezes-Filho SL, Amigo I, Prado FM, Ferreira NC, Koike MK, Pinto IFD, Miyamoto S, Montero EFS, Medeiros MHG and Kowaltowski AJ. Caloric restriction protects livers from ischemia/reperfusion damage by preventing Ca(2+)-induced mitochondrial permeability transition. Free Radic Biol Med 2017; 110: 219-227.

[35] Uzdensky AB. Apoptosis regulation in the penumbra after ischemic stroke: expression of pro- and antiapoptotic proteins. Apoptosis 2019; 24: 687-702.

[36] Favoni V, Giani L, Al-Hassany L, Asioli GM, Butera C, de Boer I, Guglielmetti M, Koniari C, Mavridis T, Vaikjarv M, Verhagen I, Verzina A, Zick B, Martelletti P and Sacco S. CGRP and migraine from a cardiovascular point of view: what do we expect from blocking CGRP? J Headache Pain 2019; 20: 27.

[37] Duan X, Yao G, Liu Z, Cui R and Yang W. Mechanisms of transcranial magnetic stimulation treating on post-stroke depression. Front Hum Neurosci 2018; 12: 215.

[38] Boonzaier J, van Tilborg GAF, Neggers SFW and Dijkhuizen RM. Noninvasive brain stimulation to enhance functional recovery after stroke: studies in animal models. Neurorehabil Neural Repair 2018; 32: 927-940.

[39] Bucur M and Papagno C. Are transcranial brain stimulation effects long-lasting in post-stroke aphasia? A comparative systematic review and meta-analysis on naming performance. Neurosci Biobehav Rev 2019; 102: 264-289.

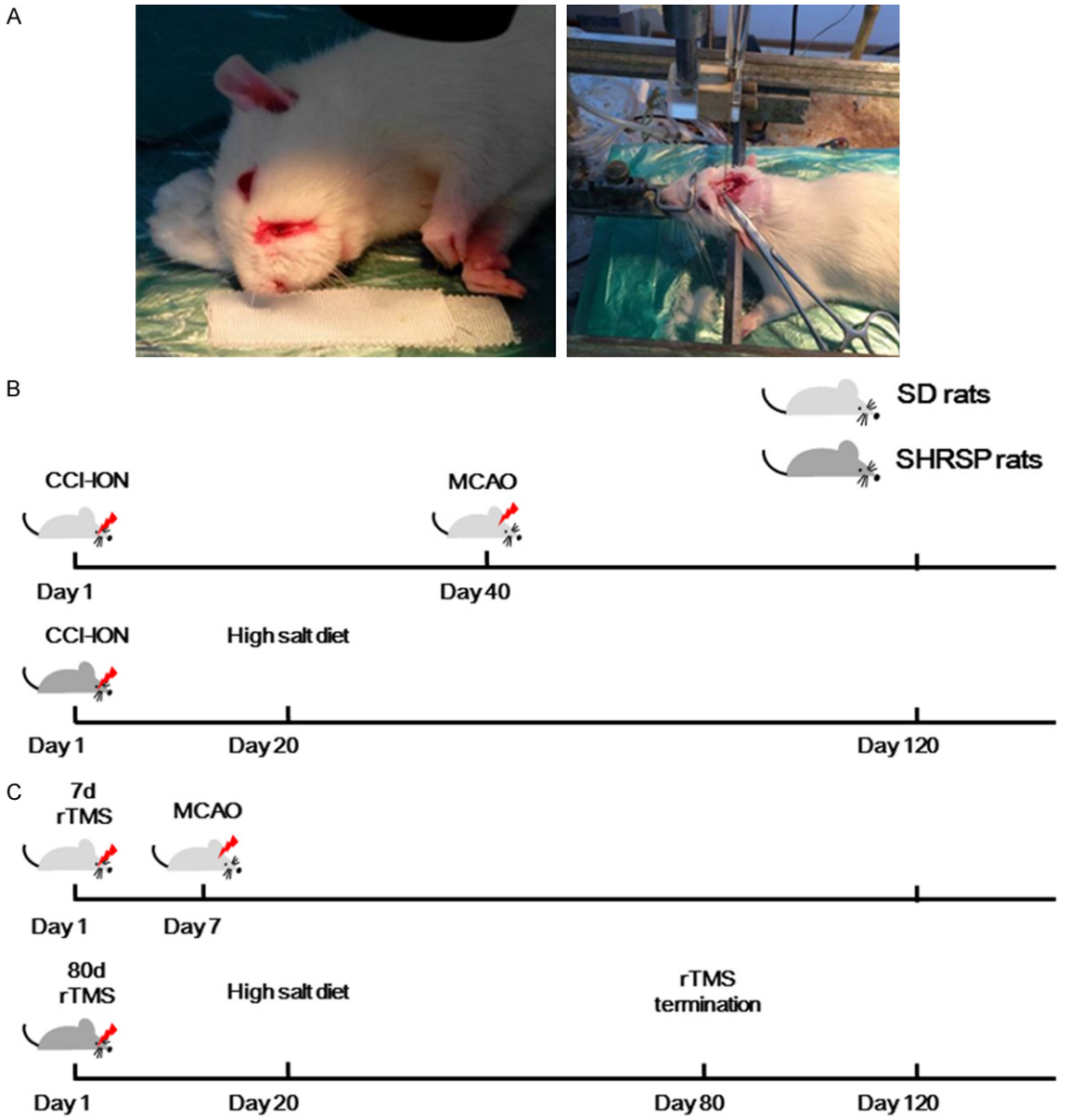

Figure S1. A. Operation diagram of CCI-ION model and microinjection via stereotaxic apparatus. B. Schematic diagram of time line of CCI-ION/MCAO model and SHRSP model. C. Schematic diagram of time line of rTMS/MCAO model and SHRSP model.

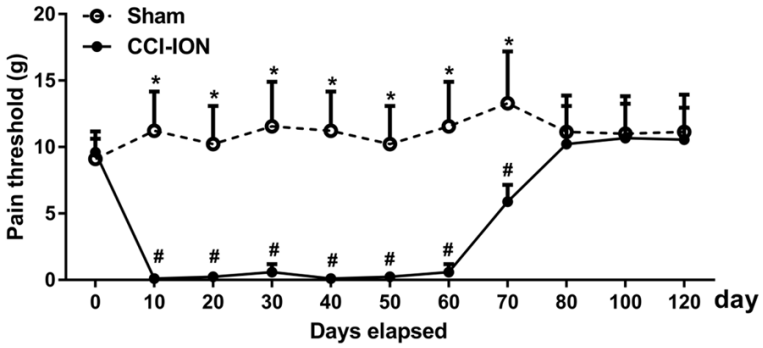

Figure S2. Continuous detection of pain threshold on rats subjected to CCI-ION or sham operation for 120 days. n=5 rats. Data are shown as mean ± SD, and analyzed by Student's t test. *P < 0.05 compared with CCI-ION group at each time point. #P < 0.05 compared with rats before CCI-ION (day 0).

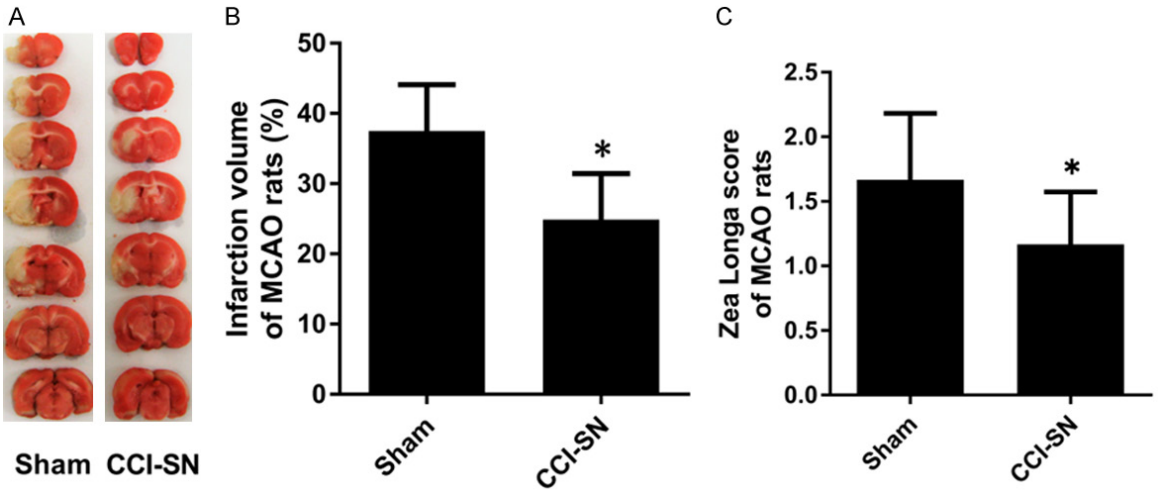

Figure S3. CCI-SN protects against stroke induced by MCAO. A, B. 2% TTC staining of coronal brain sections and quantitative analysis of the infarct volume was shown that CCI-SN significantly decreased the infarction volume than sham group. Areas of brain infarction appear white. n=5 rats. C. Zea Longa score indicated that it was decreased in CCI-SN group compared than sham group, n=5 rats. Data are shown as mean ± SD. Significance is determined by Student's t test. *P < 0.05 compared with sham group. CCI-SN: chronic constriction injury to the sciatic nerve.

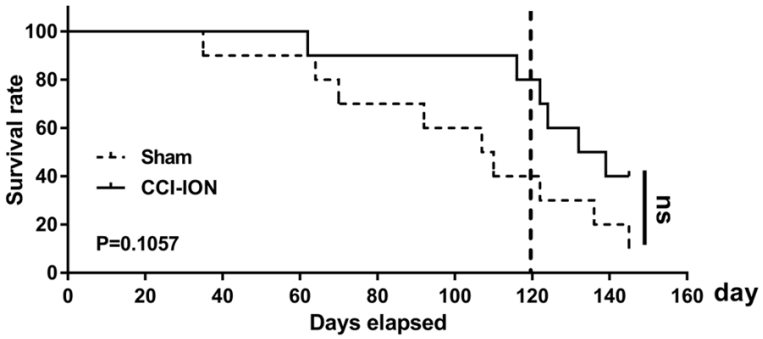

Figure S4. Survival rate of SHRSP rats subjected to CCI-ION or sham operation for 145 days. Significant differences had been found in 120 days survival rate between sham and CCI-ION group, not in 145 days survival rate. n=10 rats. Significance is determined by Log-rank (Mantel-Cox) test. ns, no significant.

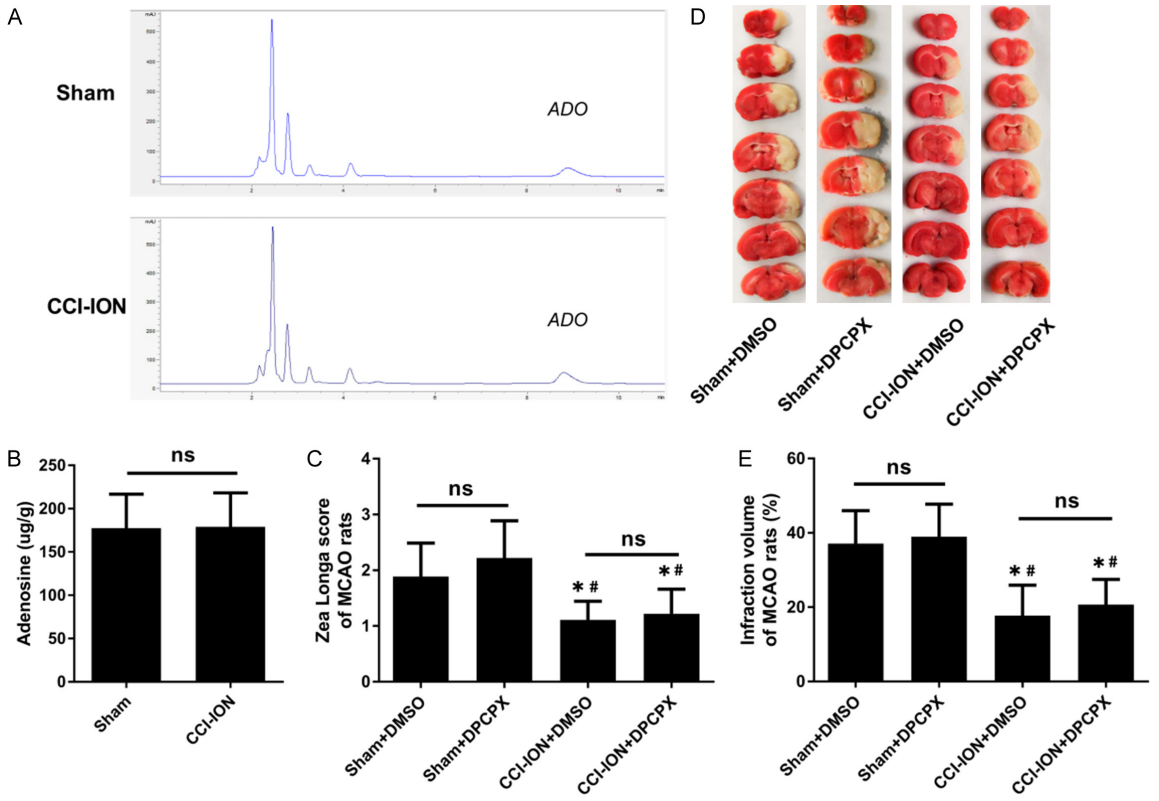

Figure S5. Adenosine (ADO) was not involved in CCI-ION induced protective effects on ischemic injuries. (A, B) The content of ADO in cortical tissues was measured by High Performance Liquid Chromatography (HPLC), which shows no significant elevation of ADO compared with sham group, n=5 rats. (C-E) Zea Longa scores, 2% TTC staining of coronal brain sections and quantitative analysis of the infarct volume between sham+DMSO and sham+DPCPX group, CCI-ION+DMSO and CCI-ION+DPCPX group had no significant differences respectively, n=5 rats. The data above were indicated that ADO was not involved in protective effect in stroke. Data are shown as mean ± SD. Significance is determined by Student's t test (B) or ANOVA followed by LSD post-hoc testing (C, E). *P < 0.05 compared with sham+DMSO group. #P < 0.05 compared with Sham+DPCPX group. ns, not signifcant.

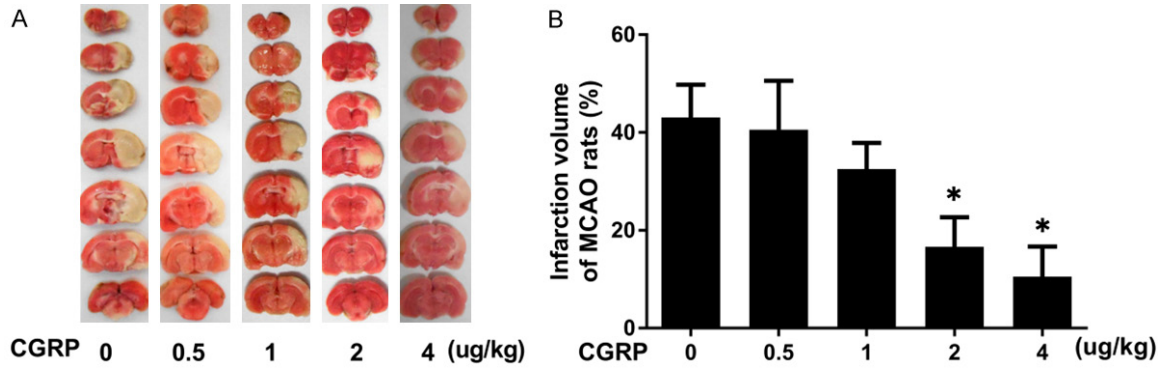

Figure S6. Effect of different doses of CGRP on MCAO induced ischemic injury. A, B. 2% TTC staining of coronal brain sections and quantitative analysis of the infarct volume were expressed that CGRP alleviated the infarct volume in a dose-dependent manner, n=5 rats. Data are shown as mean ± SD. Significance is determined by ANOVA followed by LSD post-hoc testing. *P < 0.05 compared with rats without CGRP preconditioning (0 ug/kg CGRP).

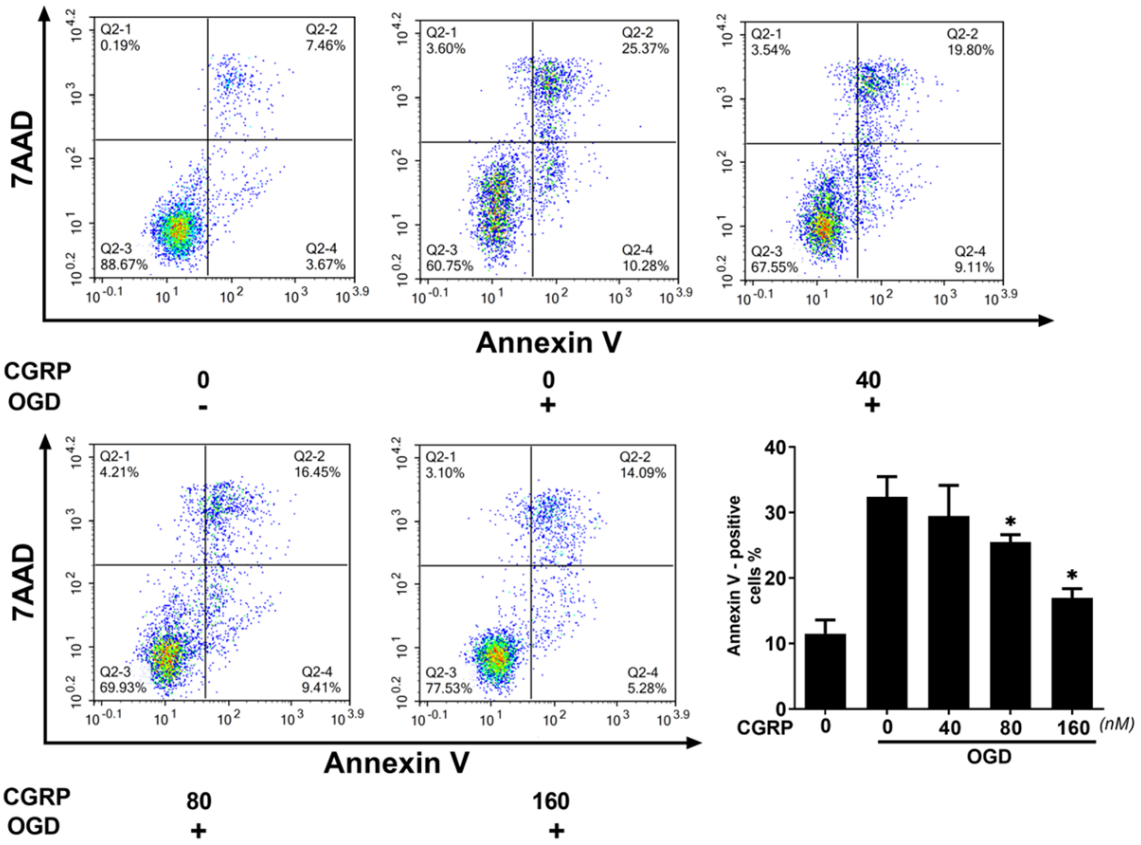

Figure S7. Effect of different doses of CGRP on neuron survival under OGD/R model. It was suggested that CGRP reduced the neuronal apoptosis in a dose-dependent manner, n=3. Data are shown as mean ± SD. Significance is determined by ANOVA followed by LSD post-hoc testing. *P < 0.05 compared with cells under OGD/R without CGRP preconditioning.